Supporting Information

Tailoring intramolecular charge transfer (ICT) dynamics for dual emission: A route to single-molecule white light emission

Sathiaraj Richard, [a] Shamla Pulath[a], Sumit Kumar*[b], and Ganesh Chandra Nandi*[a]

a. Department of Chemistry, National Institute of Technology-Tiruchirappalli, 620015, Tamil Nadu, India. E-mail: ganeshnandi@gmail.com; nandi@nitt.edu

b. Department of Chemistry, Magadh University, Bodh Gaya 824234, Bihar, India.

Table of Contents

1. Reaction Scheme for DCyDEA-OH (5) Synthesis

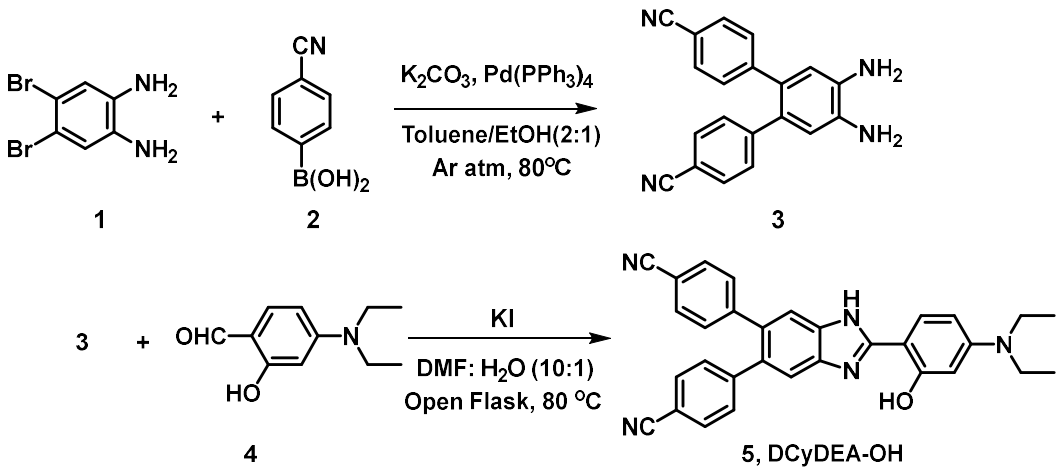

Scheme S1. Synthesis of **DCyDEA-OH (5)**

2. General Procedure for the Synthesis of 4,5-diphenylcyanobenzene-1,2-diamine (3)

A mixture of 4,5-Dibromobenzene-1,2-diamine **1** (500 mg, 1.88 mmol, 1 equiv.), 4-Cyanophenylboronic acid **2** (690.43 mg, 4.7 mmol, 2.5 equiv.), and aq. Potassium carbonate (2M solution) was dissolved in a mixture of toluene: ethanol(2:1) in a round-bottom flask under an argon atmosphere. $Pd(PPh_3)_4$ (5 mol%) was quickly added and degassed for 15 mins. The reaction mixture was heated at 80 °C for 12 hours. After completion of the reaction, the mixture was cooled, quenched with water, and extracted with DCM (3 x 20 mL). The collected organic phases were dried over Na_2SO_4, filtered, and concentrated under reduced pressure. The residue was purified by column chromatography on silica gel with 30% EtOAc in hexane as the eluent. A greenish powder of compound **3** was obtained in 71% yield.

3. (a) General Procedure for the synthesis of 4,5-diphenylcyanoimidazo-o-hydroxyphenyldiethylamine (5, DCyDEA-OH) and

The mixture of **3** (200 mg, 0.643 mmol, 1 equiv.), Diethylaminosalicylaldehyde 4 (136 mg, 0.704 mmol, 1 equiv.), and potassium iodide (107 mg,0.644 mmol, 1 equiv.) were dissolved in DMF: water (9:1) . The reaction mixture was heated at 80 °C for 8 hours in a magnetic stirrer under an open atmosphere. After completion of the reaction, the reaction was quenched with water and extracted with DCM (3 x 20 mL). The collected organic phases were dried over Na_2SO_4, filtered, and concentrated under reduced pressure and further purified using column chromatography on silica gel with 10% EtOAc in hexane as the eluent. Compound **DCyDEA-OH** was obtained as a pale-yellow powder (63% yield).

3. (b) Reaction Scheme and General Procedure for the synthesis of 4,5-diphenylcyanoimidazo-o-methoxyphenyldiethylamine (7, DCyDEA-OMe)

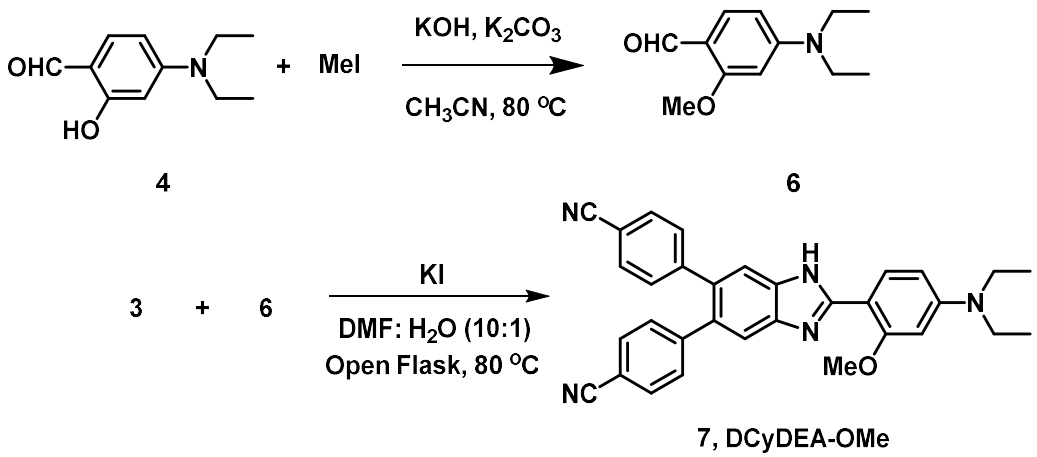

Compound **6** was synthesized following the procedure reported in the literature.[1] Subsequently, the target compound **DCyDEA-OMe (7)** was prepared using the same synthetic protocol employed for the synthesis of **DCyDEA-OH (5).**

4. Characterization Data for DCyDEA-OH (5)

Pale yellow solid (yield: 106 mg, 63%), ^{1}H NMR (500 MHz, DMSO-d_6): δ 8.015-7.997 (d, J = 9 Hz, 1H), 7.916-7.885 (t, J = 8Hz, 4H), 7.857 (s, 1H), 7.690 (s, 1H), 7.513-7.497 (d, J = 8Hz, 4H), 6.584-6.561 (dd, J = 2.5 Hz, 1H), 6.389-6.383 (d, J = 3Hz, 1H), 3.591-3.549 (q, J = 7 Hz, 4H), 1.321-1.293 (t, J = 14 Hz, 6H). ^{13}C {^{1}H} NMR (126 MHz, DMSO-d_6): δ 165.2, 160.1, 151.5, 138.0, 137.1, 136.2, 132.8, 124.0, 117.6, 114.3, 109.0, 105.3, 103.0, 49.0, 17.7. HRMS (ESI, m/z): calcd for $C_{31}H_{25}N_5O$ $(M+H)^+$: 484.2132, found: 484.2155.

5. Figure S1: ^{1}H NMR of DCyDEA-OH

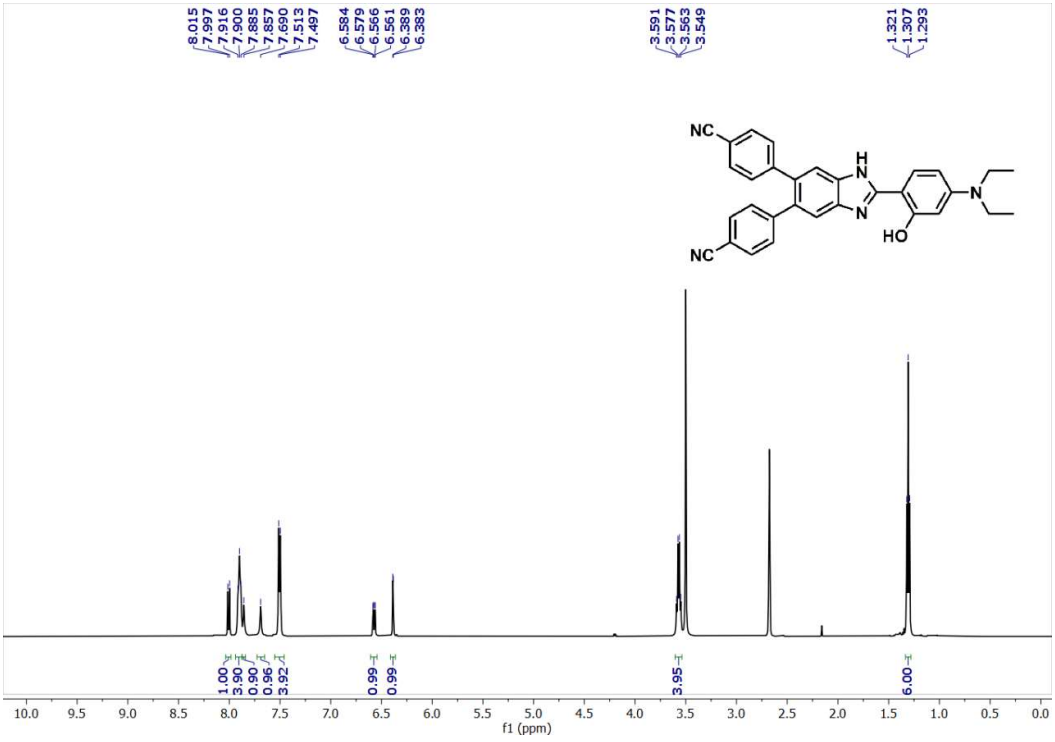

6. Figure S2: ^{13}C NMR of DCyDEA-OH

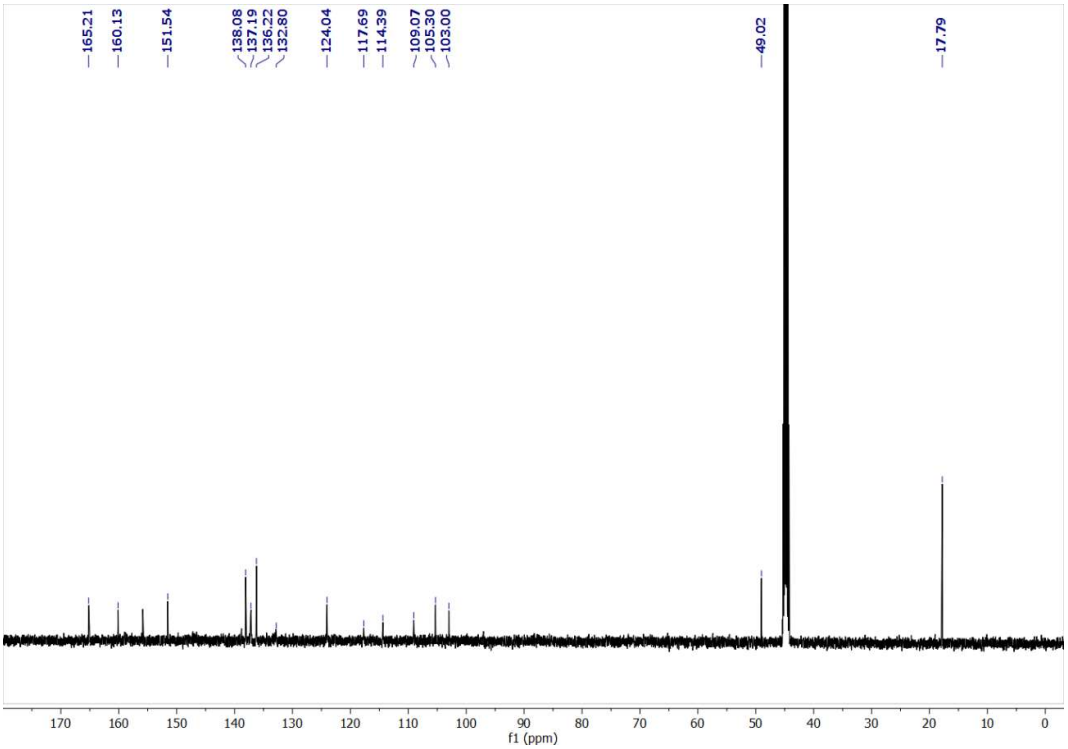

7. Figure S3: UV Vis absorption spectra of DCyDEA-OH in various solvents

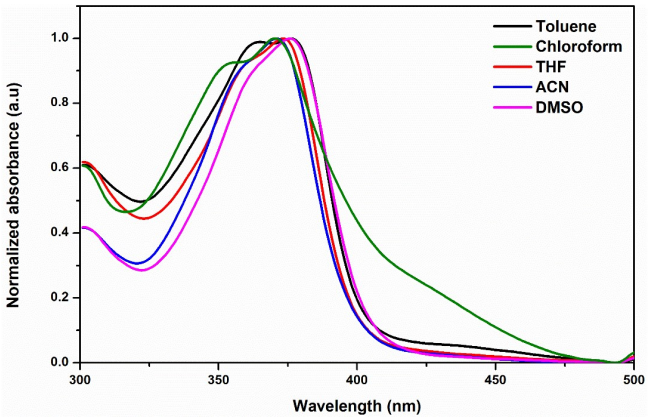

8. Figure S4: PL emission spectra of DCyDEA-OH in different solvents

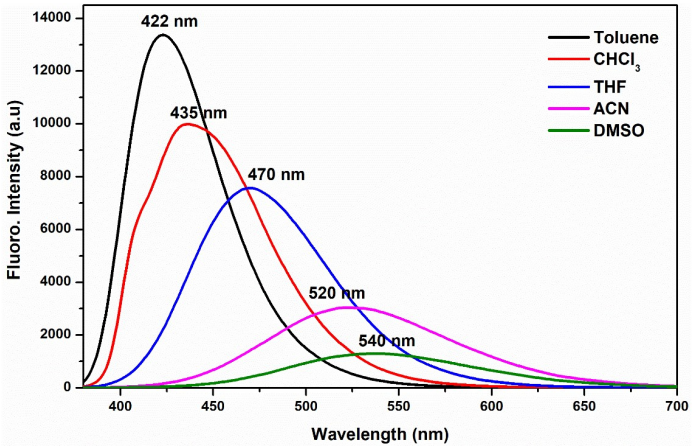

9. Figure S5: PL emission spectra of DCyDEA-OMe in different solvents

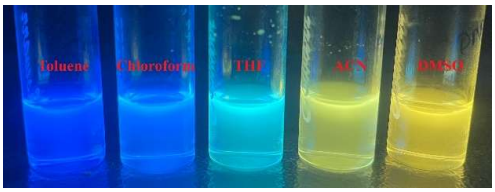

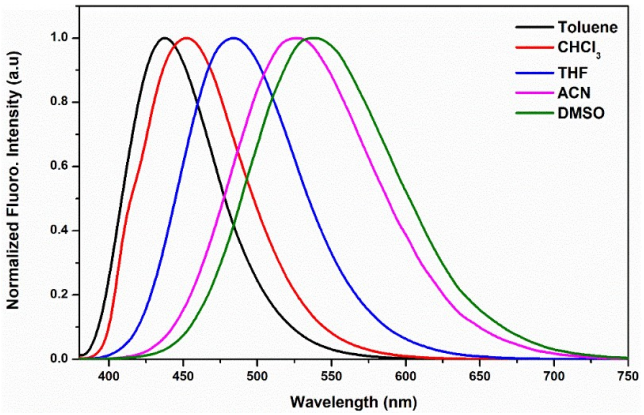

10. Figure S6: PL emission spectra (normalized) of DCyDEA-OH in different ratios of DMSO: $CHCl_3$

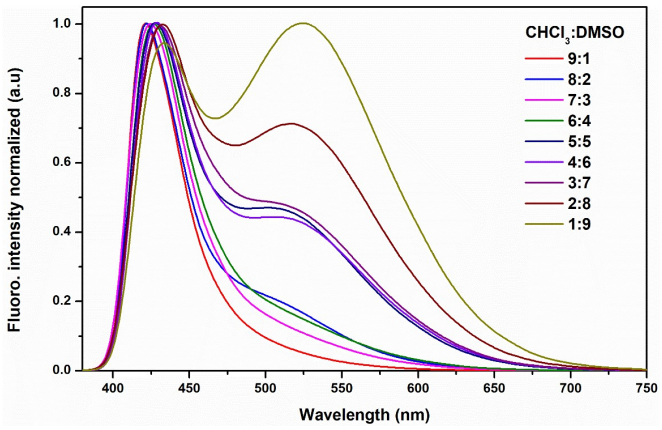

11. Figure S7 Absorbance spectrum corresponds to DCyDEA-OH in different ratios of DMSO: $CHCl_3$

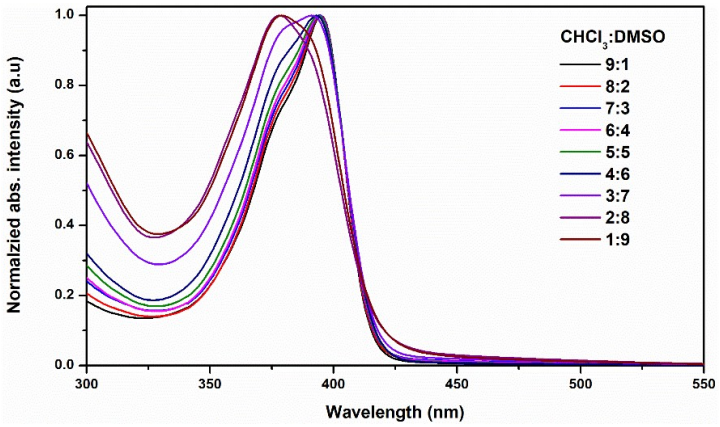

12. Figure S8: PL emission spectra (normalized) of DCyDEA-OH in DMSO with gradual addition of H^+ ion concentration

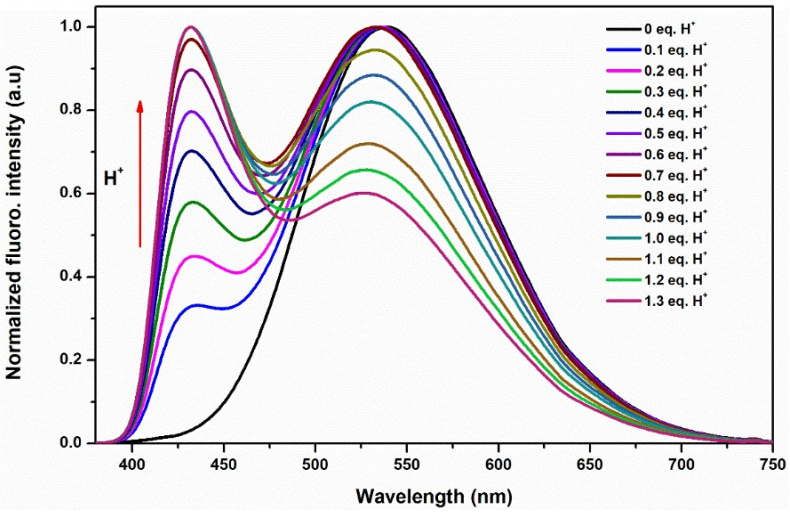

13. Figure S9 Absorbance spectrum corresponds to DCyDEA-OH in DMSO with gradual addition of H^+ ion concentration

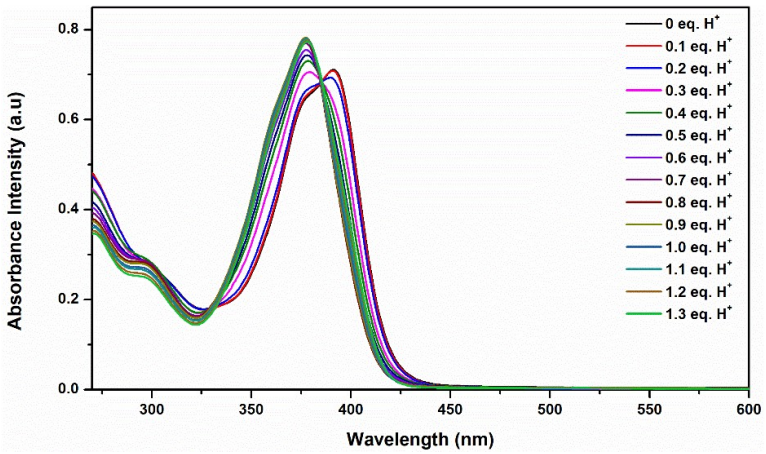

14. Figure S10 Energy level diagrams illustrating the primary transitions originating from the lowest-energy absorption bands for DCyDEA-OH

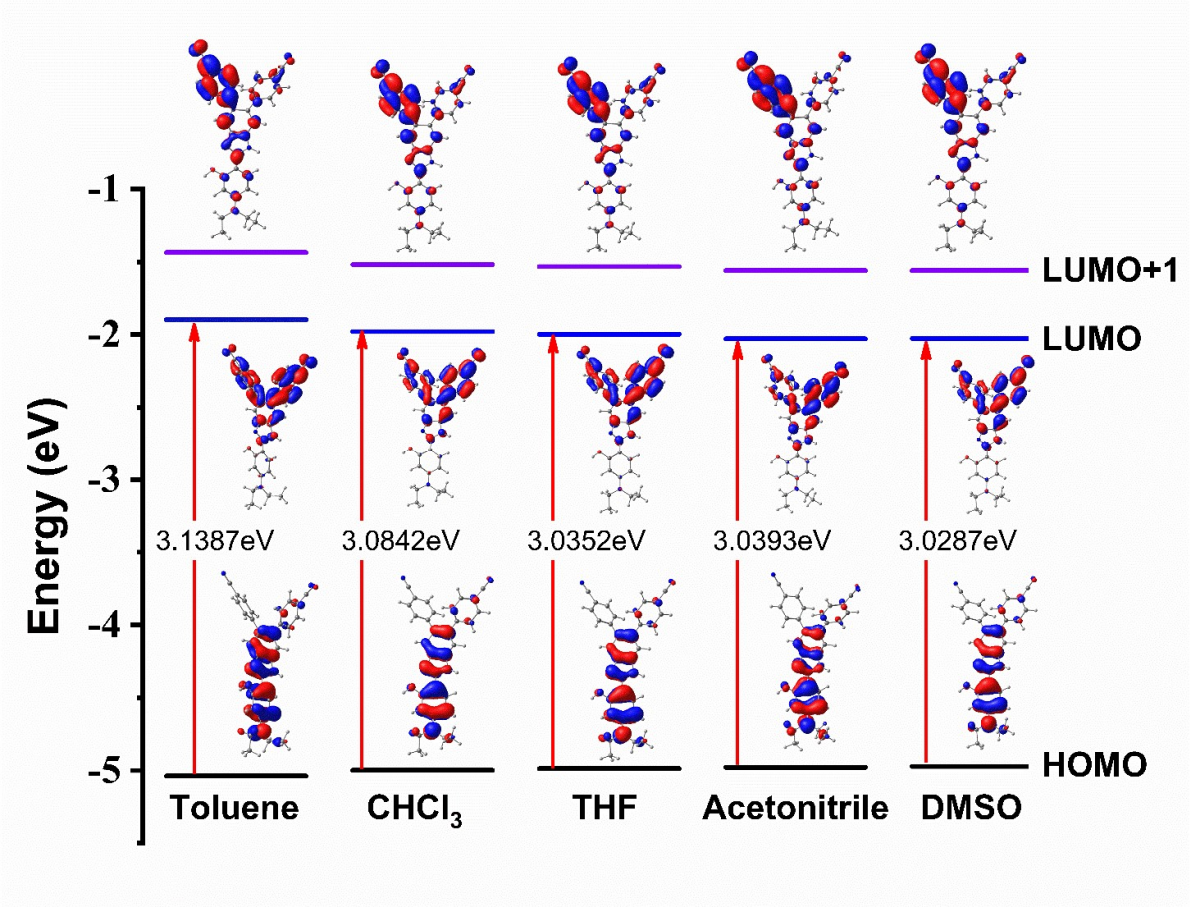

15. Quantum Yield Calculations

The quantum yield was determined with reference to quinine sulfate (QS) in 0.1 M H_2SO_4 using the following formula[2,3].

$$\Phi_{sample} = \Phi_{ref} * (OD_{ref} / OD_{sample}) * (I_{ref} / I_{sample}) * (\mu^2_{solvent} / \mu^2_{ref})$$

Where, Φ_{sample} = quantum yield of sample; Φ_{ref} = quantum yield of reference; I_{sample} = area under PL curve of sample; I_{ref} = area under PL curve of reference; OD_{ref} = absorbance of the reference; OD_{sample} = absorbance of the sample; $\mu^2_{solvent}$ = refractive index of solvent; μ^2_{ref} = refractive index of reference **(Φ_{ref} = 0.54)**

16. Additional electronic parameters of DCyDEA-OH across solvents

The electronic structure and global reactivity descriptors of DCyDEA-OH were investigated at the B3LYP/6-31G* level using the polarizable continuum model (PCM) in five solvent environments—toluene, chloroform, THF, acetonitrile, and DMSO of increasing polarity. As summarized in Table S1, solvent polarity induces systematic but modest variations in frontier orbital energies and related descriptors. With increasing dielectric constant, the HOMO undergoes greater stabilization than the LUMO, leading to a slight narrowing of the HOMO–LUMO gap (~3.1 to ~3.0 eV). This marginal band-gap reduction indicates a subtle increase in electronic softness but does not imply significant excited-state reorganization or strong charge-transfer character, consistent with the localized excitations observed in the transition density matrix analysis. Ionization energy increases slightly in polar solvents, while electron affinity decreases marginally, reflecting enhanced ground-state stabilization. Chemical hardness decreases with polarity, accompanied by a corresponding increase in softness, suggesting mildly enhanced reactivity in high-dielectric media. Electronegativity and chemical potential follow expected trends, indicating improved charge stabilization in polar environments. The electrophilicity index increases with solvent polarity, pointing to enhanced electrophilic character, though the overall solvent effect remains moderate.

Table S1: Electronic parameters of DCyDEA-OH across solvents.

Parameters	Toluene	Chloroform	THF	Acetonitrile	DMSO
LUMO (Hartree)	-0.18505	-0.18368	-0.18325	-0.1845	-0.18271
HOMO (Hartee)	-0.07131	-0.07268	-0.07332	-0.0745	-0.07441
LUMO (eV)	-5.0355	-4.9982	-4.9865	-5.0205	-4.9718
HOMO (eV)	-1.9404	-1.9777	-1.9951	-2.0272	-2.0248
I (eV)	1.9404	1.9777	1.9951	2.0272	2.0248
A (eV)	5.0355	4.9982	4.9865	5.0205	4.9718
η (eV)	-1.5475	-1.5102	-1.4957	-1.4966	-1.4735
ρ (eV)	-0.6462	-0.6621	-0.6686	-0.6682	-0.6787
χ (eV)	3.4880	3.4880	3.4908	3.5239	3.4983
CP (eV)	-3.4880	-3.4880	-3.4908	-3.5239	-3.4983
ω (eV)	-7.8615	-8.0556	-8.1473	-8.2971	-8.3055
ε (eV)	-0.6462	-0.6621	-0.6686	-0.6682	-0.6787

Starting with the frontier molecular orbitals, both HOMO and LUMO energies show systematic shifts with increasing solvent polarity. The HOMO energy decreases from –1.9404 eV in toluene to –2.0248 eV in DMSO, indicating stabilization of the ground state in polar environments. This stabilization is more pronounced for the HOMO than the LUMO, which changes from –5.0355 eV to –4.9718 eV across the same solvent gradient. These shifts suggest that while both occupied and unoccupied molecular orbitals are influenced by solvation, the polar environment more effectively stabilizes the donor (HOMO) than the acceptor (LUMO) orbitals, due to greater solute-solvent interaction with the more electron-rich HOMO.

The resulting HOMO–LUMO energy gap (ΔE) narrows slightly from ~3.1 eV in toluene to ~3.0 eV in DMSO. This marginal reduction in band gap energy with increasing polarity implies a subtle enhancement in the molecule's electronic softness and potential for electronic transitions. However, the change is not significant enough to indicate major reorganization or extensive charge-transfer character in the excited states, corroborating the interpretation from transition density matrix (TDM) analysis, discussed in the next section, where local excitations dominated without strong solvent-driven delocalization effects.

Ionization energy (I) and electron affinity (A), derived from the HOMO and LUMO energies, respectively, show complementary trends. Ionization energy increases from 1.9404 eV in toluene to 2.0248 eV in DMSO, meaning that removing an electron becomes slightly more difficult in polar media due to ground-state stabilization. Conversely, electron affinity decreases marginally, suggesting that the ability to accept an electron becomes slightly reduced.

Chemical hardness (η), which reflects resistance to charge transfer, becomes less negative from –1.5475 eV in toluene to –1.4735 eV in DMSO. This trend indicates a slight softening of the molecule in polar solvents, consistent with the band gap analysis. The corresponding increase in softness (ρ), from –0.6462 eV to –0.6787 eV, further emphasizes that **DCyDEA-OH** may become marginally more chemically reactive in higher dielectric media, though the extent of change is modest.

Electronegativity (χ), a measure of the molecule's tendency to attract electrons, slightly increases with polarity, rising from 3.4880 eV in toluene to 3.4983 eV in DMSO. The chemical potential (CP), which is the negative of electronegativity, follows the expected trend, becoming more negative with increased polarity. This reflects an increasing tendency for the molecule to stabilize additional charge in polar solvents, albeit subtly.

The electrophilicity index (ω) shows a more pronounced response to solvent effects, increasing from –7.8615 eV in toluene to –8.3055 eV in DMSO. This increase implies enhanced electrophilic character in more polar solvents, as a result of increased electron withdrawal capacity and reduced hardness. This trend could have implications in solvent-tuned reactivity for electrophilic reactions or binding affinity to nucleophilic targets, making **DCyDEA-OH** a better electron acceptor in polar solvents.

Thus, the data demonstrate that solvent polarity has a tangible, though not drastic, effect on the electronic and reactivity parameters of **DCyDEA-OH**. The molecule becomes slightly softer, more electrophilic, and exhibits a narrower band gap in polar solvents. These effects are consistent with modest polar solvation and stabilization mechanisms, yet they do not suggest significant charge-transfer character in the excited states. This observation aligns well with the localized excitation behavior noted in TDM analysis and the minimal shift in UV absorption spectra, thus presenting **DCyDEA-OH** as a molecule with reasonably solvent-robust optoelectronic characteristics.

17. Transition dipole moment of DCyDEA-OH across solvents:

The data reported in Table S2 in the supporting information provides a detailed insight into the excited-state properties of DCyDEA-OH in various solvents with differing dielectric constants. The three critical sets of parameters—electric dipole moments, magnetic dipole moments, and velocity dipole moments—offer a multidimensional understanding of the nature and behavior of electronic transitions. These quantities are crucial for interpreting absorption and emission properties, characterizing transition moments, and predicting how the molecule will respond to external electromagnetic fields, particularly in diverse solvation environments.

Table S2: Excited state transition electric dipole moments of DCyDEA-OH in different solvent.

Solvent	Dielectric Constant	excited state transition electric dipole moments (a.u.)			excited state transition magnetic dipole moments (a.u.)			excited state transition velocity dipole moments (a.u.)		
		x	y	z						
Toluene	2.38	-2.4631	1.1876	0.1306	-0.0119	-0.0724	0.2581	0.242	-0.1179	-0.0133
		3.1887	0.1809	0.0002	0.0457	0.0382	-0.0016	-0.3558	-0.0206	-0.0001
Chloroform	4.81	2.4641	1.1774	-0.1235	0.0132	-0.0758	-0.2704	-0.2365	-0.114	0.0123
		-3.1814	0.1564	0.0047	-0.0471	0.0469	0.0166	0.3485	-0.0176	-0.0005
THF	7.58	-2.4643	1.1677	0.1203	-0.0111	-0.0741	0.2745	0.2342	-0.112	-0.0118
		3.1625	0.1438	-0.0071	0.0478	0.047	-0.0231	-0.344	-0.0162	0.0007
Acetonitrile	35.94	2.428	1.1464	-0.1202	0.0115	-0.0714	-0.2729	-0.228	-0.1087	0.0117
		3.1205	-0.1218	-0.0052	0.0478	-0.0453	-0.0256	-0.3365	0.0137	0.0005
DMSO	46.7	-2.5462	1.1794	0.1115	-0.0145	-0.0892	0.286	0.2383	-0.1114	-0.0106
		-3.1879	-0.1431	0.0118	-0.0495	-0.0713	0.0257	0.3426	0.016	-0.0012

18. Excited-State Electric Dipole Moments of DCyDEA-OH across solvents

The excited-state transition electric dipole moments represent the net change in dipole moment upon electronic excitation, and they serve as a direct measure of the extent of charge redistribution within the molecule. These vectors (x, y, z components) show solvent-dependent variations, primarily in the x-direction. In all solvents, the x-components are consistently dominant compared to the y- and z-components, reaffirming that the intramolecular charge transfer (ICT) character of the excited state is oriented predominantly along the molecular x-axis, which could correspond to the molecular long axis in a planar π-conjugated system.

Interestingly, a comparison between low-polarity (toluene, $\varepsilon = 2.38$) and high-polarity (DMSO, $\varepsilon = 46.7$) solvents reveals significant changes in the dipole magnitude and even direction (sign reversal), particularly in the x-component. This behavior indicates that the electronic structure of the excited state is highly sensitive to solvation, with polar solvents stabilizing charge-separated states more effectively. Such changes are expected due to differential stabilization of frontier molecular orbitals (e.g., HOMO and LUMO) in polar media, which alters their spatial distribution and energy gaps, ultimately modifying the transition dipole orientation and magnitude.

19. Excited-State Magnetic Dipole Moments of DCyDEA-OH across solvents

The excited-state magnetic dipole moments provide insight into the angular momentum characteristics of the excited-state transitions. The z-component of the magnetic dipole moment stands out across all solvents, particularly in nonpolar toluene (0.2581 a.u.) and in DMSO (0.286 a.u.), suggesting the involvement of out-of-plane $\pi \rightarrow \pi^*$ transitions, which are common in planar aromatic systems.

The y- and x-components of magnetic dipole moments show variations in sign and magnitude across solvents and transitions, indicating a change in transition symmetry and orbital overlap with solvent polarity. For instance, a switch from negative to positive magnetic moment values in the x-component for the second transition in THF and acetonitrile reflects the change in the magnetic orientation of transition density matrices. These observations imply that the solvent not only affects energetic alignment but also modifies the spatial nature of electronic excitations.

20. Excited-State Velocity Dipole Moments of DCyDEA-OH across solvents

Velocity dipole moments, derived from the time-dependent formulation of transition dipole moments, are especially relevant in calculating oscillator strengths and transition probabilities. Across the solvents, the x-component remains dominant and consistent in sign with the corresponding electric dipole component, supporting the reliability of the computed transitions.

The magnitude of the velocity dipole also responds to solvent polarity. In more polar solvents (e.g., DMSO and acetonitrile), while the absolute values of the x-component decrease slightly compared to less polar solvents, the direction and proportion among x, y, and z components remain preserved.

21. Charge Analysis (Natural Population Analysis (NPA)

The Natural Bond Orbital (NBO) charge analysis (Table S3) of DCyDEA-OH across solvents of varying dielectric constant demonstrates how solvent polarity profoundly influences intramolecular electronic distribution, which in turn correlates with experimentally observed UV-Vis excitation shifts.

In low dielectric media such as Toluene ($\varepsilon = 2.38$), the charge separation is comparatively less pronounced. Atoms such as nitrogen (19N, 21N, 29N, and 37N) and the key oxygen (28O) still maintain high electronegativity, but with slightly lower negative charge values compared to polar solvents. For instance, the charge on 21N increases from −0.5701 in DMSO to −0.5776 in Toluene, and oxygen atom 28O changes from −0.6859 in Acetonitrile to −0.6712 in Toluene. This subtle reduction in polarity correlates with a shorter excitation wavelength ($\lambda max = 415$ nm), reflecting a larger HOMO–LUMO energy gap due to reduced stabilization of the excited state in a non-polar environment.

As the dielectric constant increases—from Chloroform ($\varepsilon = 4.81$) to THF ($\varepsilon = 7.58$)—the molecule shows progressively greater polarization. NBO charges on key donor and acceptor atoms become slightly more negative (for electron-rich centres) or more

positive (for proton donors), indicating enhanced charge separation facilitated by the polar medium. This leads to increased stabilization of charge-transfer states, which is consistent with the red shift in UV-Vis spectra (from 441 nm in Chloroform to 459 nm in THF).

In highly polar solvents such as Acetonitrile (ε = 35.94) and DMSO (ε = 46.7), this effect becomes even more pronounced. The stabilization of electron-rich centres—especially 21N and 28O—is reflected in their more negative NBO charges (e.g., −0.5701 and −0.6849 in DMSO, respectively). Such strong dipolar stabilization narrows the HOMO–LUMO gap, resulting in significantly red-shifted absorption maxima (520 nm in Acetonitrile and 539 nm in DMSO). This shift supports the idea that solvation in polar media preferentially stabilizes the excited state more than the ground state, leading to lower energy transitions.

This trend highlights a clear correlation that as the dielectric constant of the solvent increases, the degree of intramolecular charge separation also increases, enhancing dipole moment differences between ground and excited states. Consequently, this increases solvent-induced stabilization of excited states, which is directly manifested as red shifts in the UV-Vis spectra.

Table S3: The Natural Bond Orbital (NBO) charge analysis of DCyDEA-OH across solvents.

Atom	Solvent				
	Acetonitrile	Chloroform	DMSO	THF	Toluene
1C	-0.06058	-0.05744	-0.06097	-0.05876	-0.05461
2C	-0.05327	-0.05433	-0.05334	-0.05399	-0.0546
3C	-0.22436	-0.21916	-0.22496	-0.22118	-0.21515
4C	0.13156	0.13267	0.13191	0.13237	0.13324
5C	0.13773	0.13866	0.13804	0.13841	0.13896
6C	-0.23446	-0.23779	-0.23502	-0.23677	-0.23965
7C	-0.02001	-0.02167	-0.01974	-0.02091	-0.02369
8C	-0.02585	-0.02589	-0.02579	-0.02576	-0.02659
9C	-0.2227	-0.22106	-0.22295	-0.22172	-0.21974
10C	-0.17638	-0.17636	-0.17638	-0.1763	-0.17674
11C	-0.19975	-0.19489	-0.20009	-0.19686	-0.19017
12C	-0.17596	-0.17686	-0.17597	-0.17651	-0.17772
13C	-0.2287	-0.23	-0.22873	-0.22954	-0.23072
14C	-0.22658	-0.22673	-0.22668	-0.22671	-0.22681
15C	-0.17466	-0.17595	-0.17458	-0.17545	-0.17703
16C	-0.19638	-0.1928	-0.1966	-0.1943	-0.18899
17C	-0.17626	-0.17687	-0.17625	-0.17662	-0.17752

18C	-0.21817	-0.21756	-0.21818	-0.21776	-0.21709
19N	-0.52116	-0.50526	-0.52217	-0.51129	-0.49245
20C	0.42127	0.42105	0.42003	0.42092	0.42108
21N	-0.57103	-0.57429	-0.57014	-0.57298	-0.57759
22C	-0.21987	-0.21354	-0.22001	-0.21593	-0.20832
23C	0.39172	0.39507	0.39221	0.39406	0.39695
24C	-0.38289	-0.38147	-0.3833	-0.38216	-0.37992
25C	0.22093	0.22017	0.22132	0.2206	0.21895
26C	-0.31537	-0.31479	-0.31518	-0.31504	-0.31416
27C	-0.18197	-0.18152	-0.18047	-0.18134	-0.1821
28O	-0.68588	-0.67713	-0.68486	-0.68	-0.67123
29N	-0.42461	-0.42779	-0.42372	-0.42634	-0.43107
30C	-0.25591	-0.25559	-0.257	-0.25606	-0.25462
31C	-0.26166	-0.26118	-0.26175	-0.26141	-0.26063
32C	-0.69849	-0.6976	-0.69805	-0.6978	-0.697
33C	-0.68947	-0.68923	-0.68896	-0.68913	-0.68937
34C	0.30937	0.30006	0.30972	0.30377	0.29128
35N	-0.3786	-0.36036	-0.37946	-0.36768	-0.343
36C	0.31506	0.30524	0.31551	0.30918	0.29599
37N	-0.3752	-0.35874	-0.3759	-0.3654	-0.34265
38H	0.25221	0.25226	0.25211	0.25228	0.252
39H	0.25222	0.24753	0.25232	0.24923	0.24413
40H	0.25721	0.25642	0.25723	0.25674	0.25563
41H	0.25906	0.25752	0.25908	0.25813	0.25603
42H	0.25916	0.2567	0.25922	0.25763	0.25463
43H	0.25293	0.24984	0.25308	0.251	0.24737
44H	0.25668	0.2543	0.25685	0.25527	0.25203
45H	0.26048	0.25804	0.26057	0.25899	0.25588
46H	0.26018	0.25805	0.26025	0.25888	0.25618
47H	0.2582	0.25644	0.25829	0.25712	0.25497
48H	0.45458	0.44784	0.45376	0.45015	0.44312
49H	0.24411	0.23893	0.24432	0.24093	0.23466
50H	0.24375	0.24018	0.24424	0.24162	0.23717
51H	0.23855	0.23341	0.23696	0.23481	0.2313
52H	0.50849	0.50249	0.50843	0.50473	0.49747
53H	0.24629	0.24431	0.24672	0.24521	0.24232
54H	0.23866	0.23752	0.23914	0.23805	0.23644
55H	0.23329	0.23147	0.23431	0.2325	0.22921
56H	0.23795	0.23636	0.23713	0.23666	0.23557
57H	0.2543	0.25354	0.25452	0.25392	0.25262
58H	0.2386	0.23808	0.23836	0.23816	0.23782
59H	0.23748	0.23654	0.23753	0.23695	0.23555
60H	0.23779	0.23663	0.23797	0.23707	0.23572

61H	0.23418	0.23528	0.23408	0.23484	0.23631
62H	0.23219	0.23127	0.23201	0.23159	0.23034

22. References

(1) J. K. Wang, C. H. Wang, C. C. Wu, K. H. Chang, C. H. Wang, Y. H. Liu, C. T. Chen, P.T. Chou, *J. Am. Chem. Soc*. **2024**, 146, 5, 3125–3135

(2) Q. Zhang, Y. Gao, S. Zhang, J. Wu, H. Zhou, J. Yang, X. Tao, Y. Tian, *Dalton Trans*, **2012**, 41, 7067.

(3) J. E. Murphy, M. C. Beard, A. G. Norman, S. P. Ahrenkiel, J. C. Johnson, P. Yu, O. I. Micic, R. J. Ellingson, A. J. Nozik, *J. Am. Chem. Soc*, **2006**, 128, 3241.